The Seventh Asian-Pacific Symposium on Structural Reliability and Its Applications (APSSRA2020)
October 4–7 2020, Tokyo, Japan
T. Takada, I. Yoshida & T. Itoi (editors)

Wireless Seismic Response Control of an Instrument with Casters Based on Reinforced Learning Considering Stochastic Models of Computer Vision

K. Wakabayashi[1], M. Kohiyama[2], R. Eguchi[3] and M. Takahashi[2]

[1]*Graduate Student, Graduate School of Science and Technology, Keio University. Email: 61521201@keio.jp*
[2]*Professor, Department of System Design Engineering, Faculty of Science and Technology, Keio University.*
[3]*Graduate Student, Graduate School of Science and Technology, Keio University*

Abstract: We developed a computer-vision-based system to control the response of medical instruments with casters in a building subjected to earthquake excitation. The controller employed a neural network, and reinforced learning based on the dynamic simulations of a controlled instrument under building floor motion was conducted. In the dynamic simulations, we used the Open Dynamics Engine, which is a simulator library of three-dimensional rigid body dynamics and introduced a friction model to simulate the dynamic behavior of the casters. To accurately simulate the dynamic behavior of the controlled instrument, we considered the control delay of the proposed system and introduced stochastic models of errors to identify the displacement of the instrument using computer vision. To validate the proposed system, we performed dynamic simulations of a controlled instrument under building floor motion. It was revealed that the instrument response was significantly suppressed by introducing the stochastic model of errors in the training of NN. This result suggests the usefulness of stochastic models in enhancing the performance of reinforced learning based on dynamic simulations.

Keywords: wireless communication, neural network, reinforcement learning, medical instruments, shaking table test.

1. Introduction

When a large earthquake occurs, medical facilities that will serve as disaster medical centers in the region must take measures to maintain function and prevent damage to expensive precision instruments. This can be achieved by protecting essential instruments using seismic isolation devices and fixing instruments that are expected to be agitated by the shaking. However, introducing seismic isolation devices after constructing buildings and securing instruments that cannot be fixed are challenging tasks. As a result, in case of an earthquake, the function of a medical facility will not be maintained due to the damage to or breakdown of precision instruments, and medical activities such as emergency lifesaving activities will be seriously hindered. We developed a computer-vision-based system to control the response of a medical instrument with casters in a building subjected to earthquake excitation (Wakabayashi et al. 2020). The controller employs a neural network (NN), and the reinforced learning is conducted based on dynamic simulations of a controlled instrument under building floor motion. In the dynamic simulations, we used the Open Dynamics Engine (ODE), which is a simulator library of three-dimensional rigid body dynamics; we introduced a friction model to simulate the dynamic behavior of the casters. In this study, to accurately simulate the dynamic behavior of the controlled instrument, we considered the control delay of the proposed system and introduced stochastic models of accuracy to identify the displacement of the instrument using computer vision.

2. Proposed Control Method

We proposed a control method that uses computer vision and wireless communication, as shown in Fig. 1, assuming an instrument with casters in a building (Wakabayashi et al. 2020). The proposed method can control an instrument using an existing security camera in the facility.

The control was performed using an instrument that can switch the casters between fixed and non-fixed conditions using an electromagnet based on the difference in friction between the fixed and non-fixed states. In this method, an augmented reality (AR) marker on the instrument was monitored by the camera, as shown in Fig. 1, and the video image is transmitted to the computer by serial communication. Next, the computer identified the posture information (displacement and tipping angle) of the instrument. Through a predetermined formula, the computer input the identified posture information to the NN, determined whether the casters are fixed or non-fixed, and output a switching command to control the electromagnet. Finally, the switching command was transmitted to the switching device via wireless communication to operate the caster control instrument.

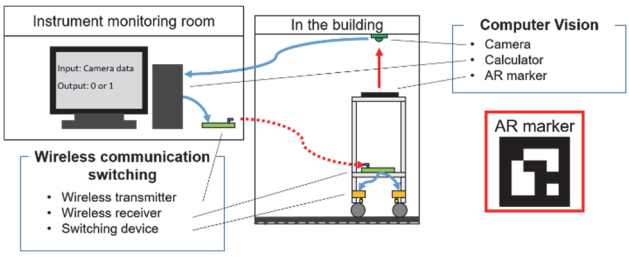

Figure 1. Schematic of the proposed method.

3. Models of Building and Instrument with Casters

3.1 Building model

The building model assumes linear elasticity. The equation of the building motion can be expressed by the following equation:

$$\mathbf{M}_b\ddot{\mathbf{X}}_b + \mathbf{C}_b\dot{\mathbf{X}}_b + \mathbf{K}_b\mathbf{X}_b = -\mathbf{M}_b\ddot{\mathbf{U}}, \quad (1)$$

where $\mathbf{M}_b$ is a building mass matrix, $\mathbf{C}_b$ is a damping matrix, $\mathbf{K}_b$ is a stiffness matrix, $\mathbf{X}_b$ is a relative displacement vector from the ground and $\mathbf{U}$ is an absolute

displacement vector on the ground. Each parameter is set as follows: The mass m_{bi} of each floor of the building is 1.0×10^6 kg, and the floor height $H_{\mathrm{b}i}$ of each floor is 3.5 m. The horizontal stiffness coefficient $K_{\mathrm{b}i}$ of the i-th floor of the building is assumed to have all stories uniformly deformed by the seismic force that follows the A_i distribution designated by the Building Standard Law of Japan. In this study, we assumed a 5-floor steel-framed building, and the fundamental natural period of the model was calculated to match the design-use fundamental natural period $T_1 = 0.529$ s given by the following equation.

$$T_1 = (0.03 \text{ s/m}) \times h_{\mathrm{b}}, \tag{2}$$

where h_{b} is the height of the building. The damping is assumed to be a stiffness proportional type.

$$\mathbf{C}_{\mathrm{b}} = \frac{2\zeta_{\mathrm{b}}}{\omega_{\mathrm{b}}}\mathbf{K}_{\mathrm{b}}, \tag{3}$$

where ζ_{b} is the first-mode damping factor of the building and ω_{b} is the first-mode natural circular frequency of the building. The value of ζ_{b} is assumed to be 0.02.

3.2 Model of the instrument with casters

In this study, we conducted shaking table tests for the table motion of a simulated floor response. We used a two-stage "silent wagon" (or low-noise casters) made by Matsuyoshi Medical Instrument that is actually used in medical facilities as an instrument with casters to carry a medical appliance. Figure 2 shows a photograph of the instrument with casters. The casters of this instrument rotate by a swivel; however, for simplicity, in this study, the swivel was fixed and processed, ensuring that the wheels roll in only one direction. The model of the instrument with casters is shown in Fig. 3, and the variables are defined in Table 1. The instrument with casters is considered to be a rigid body composed of 10 parts: two shelf boards, four columns and four casters. In addition, the difference between the fixed and non-fixed casters is expressed by the difference in friction in the numerical model.

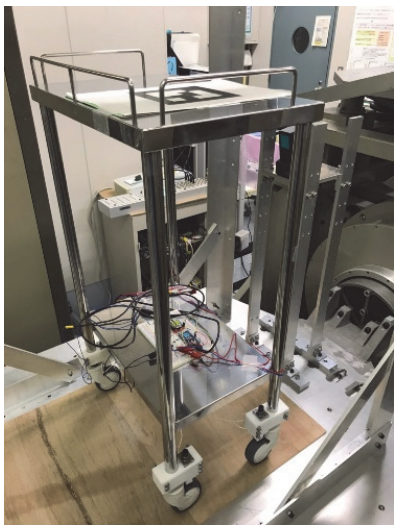

Figure 2. Instrument with casters.

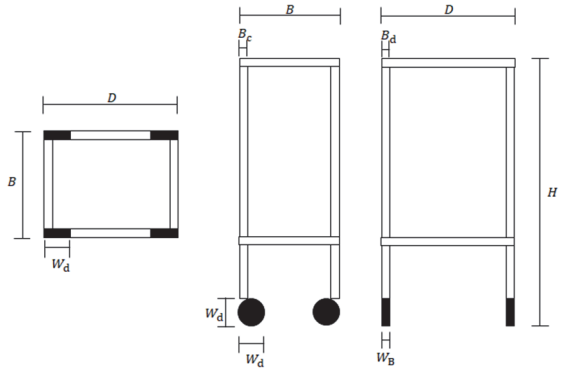

Figure 3. Model of the instrument with casters.

Table 1. Parameters of the model of the instrument with casters.

Specifications	Variable	Value
Total width	B	0.30 m
Total depth	D	0.40 m
Total height	H	0.72 m
Total mass	M	4.96 kg
Width of pillar	B_{c}	0.025 m
Pillar depth	D_{c}	0.025 m
Pillar height	$H - W_{\mathrm{d}}$	0.64 m
Mass of one pillar	M_{c}	0.21 kg
Shelf width	B_{t}	0.30 m
Shelf depth	D_{t}	0.40 m

4. Stochastic Models of the Displacement of Instrument Using Computer Vision and Delay of the Proposed System

4.1 Stochastic models of the displacement of instruments using computer vision

In our previous study, we observed that the tipping angle of the instrument insignificantly affected the control performance (Wakabayashi et al. 2020). Thus, we focus on the displacement of the instrument. The equation to identify stochastic models of the displacement of the instrument using computer vision is as follows.

$$d_C = d_L + \Delta d, \tag{4}$$

where d_C represents the displacement of the instrument identified by computer vision, d_L is the displacement of the instrument measured by a laser displacement meter (assumed as truth), and Δd is the difference between d_C and d_L, which is assumed to be the error. To derive the stochastic models of Δd, we conducted shaking table tests by inputting the table motion of a simulated floor response of a building under the ground acceleration of the Taft NS wave scaled to have the maximum velocity of 25 cm/s. (Fig. 4)

Figure 5 shows a histogram of Δd. The mean of Δd, $\mu = -0.0022$ m, however, was extremely small, and there was no reasonable source of the non-zero mean. Thus, we considered the zero-mean model. The standard deviation of Δd was $\sigma = 0.0247$ m and kurtosis of Δd was $K_w = 2.8103$. Based on this kurtosis value, we employed Laplace distribution with a kurtosis of 3 as the stochastic model of Δd.

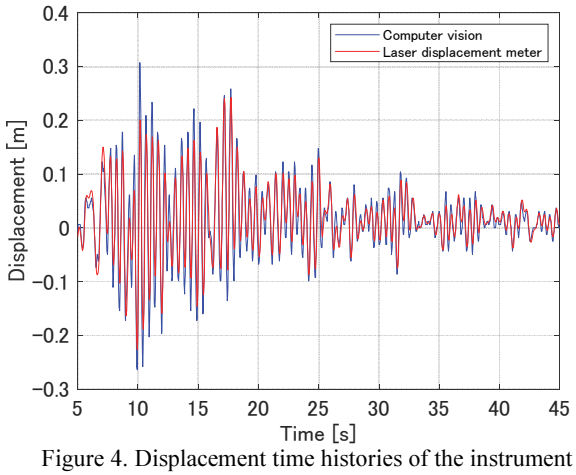

Figure 4. Displacement time histories of the instrument measured by computer vision and a laser displacement meter (5–45 s).

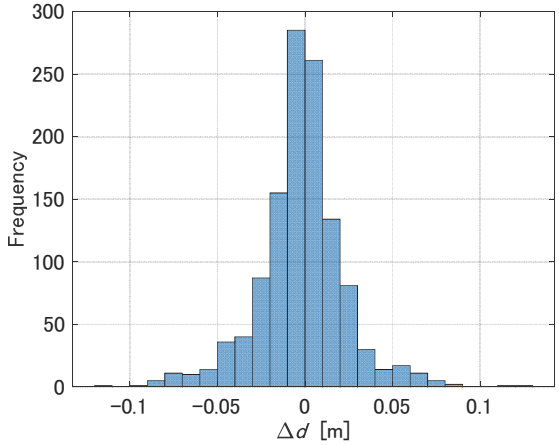

Figure 5. Histogram of the displacement measurement error Δd.

4.2 Delay of the proposed system

The equation for the delay of the proposed system is as follows.

$$t_d = t_i + t_c + t_s, \tag{5}$$

where t_d represents the entire delay of the proposed system, t_i (0.275 s) is the delay caused by the serial communication between the camera and the video image transmitted to the computer, t_c (0.033 s) is the delay of calculation for identifying posture information and outputting the switching command based on NN, and t_s (1.342 s) is the delay of the activated switching device via wireless communication. Therefore, the total t_d was 1.650 s.

5. Seismic Response Analysis of the Instrument with Casters

5.1 Seismic response analysis of the instruments with casters using ODE

The physics engine ODE for rigid body analysis was used for the seismic response analysis of instruments with casters. Saomoto and Yoshimi (2013) simulated the seismic response of the furniture using ODE and verified the accuracy of the friction model by implementing energy balance in a sliding-cube model. When the time step Δt was 0.01 s and the friction coefficient was 0.4 or less, the relative error of the friction coefficient calculated from the set value of the friction coefficient and the sliding distance was 3% or less on average; the accuracy can be improved by decreasing the time step. In this study, to obtain higher accuracy, numerical analysis was performed with a time step Δt of 0.001 s. Moreover, we simulated the dynamic behavior of the instrument using the friction model (Wakabayashi et al. 2020).

5.2 Introduction of the stochastic models into dynamic analysis

We introduced stochastic models into the dynamic analysis to reproduce the displacement of the instrument identified by computer vision.

$$d_{Csim} = d_{sim} + \Delta d_{sim}, \tag{6}$$

where d_{Csim} represents the displacement with identification error to reproduce the displacement of the instrument identified by computer vision, d_{sim} is the displacement calculated by the seismic response analysis of the instrument with casters and Δd_{sim} is the identification error, which is given by random numbers following the constructed Laplace distribution. Figure 6 depicts the histogram of Δd_{Csim}. The kurtosis of Δd_{Csim}, K_w, and standard deviation of Δd_{Csim}, σ, are 3.0196 and 0.0247 m, respectively and satisfactorily agree with the experimental values 2.8103 and 0.0247 m, respectively. Therefore, we confirmed that Δd_{Csim} successfully simulated the displacement of the instrument identified via computer vision.

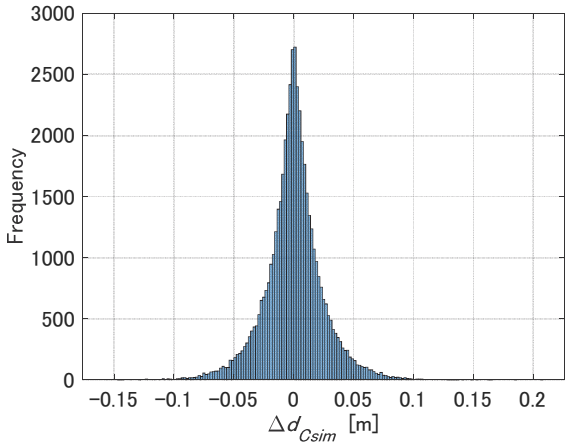

Figure 6. Histogram of the simulated displacement measurement error Δd_{Csim}.

6. Switching Control Design

6.1. Switching-control algorithm

In the proposed method, the motion control of the instrument was performed by switching between fixed and non-fixed casters of the instrument with casters. Therefore, it is important to identify the moment when the caster is fixed and non-fixed. In this study, NN-based reinforcement learning was used to design the switching conditions. Figure 7 shows a schematic diagram of the NN, where **x**, **m** and **y** are vectors that represent the input, middle and output layers, respectively, **W** is a matrix that represents the weight, and h the number of middle layers. In

addition, conversion by the activation function was performed at locations marked with "circle → square" in the middle layer. In this study, we used a rectified linear unit (ReLU), which is often used in NN. If the argument of a function $\mathrm{ReLU}(x) = \max(0, x)$ is a vector, then the maximum operation above was performed for each element of the vector.

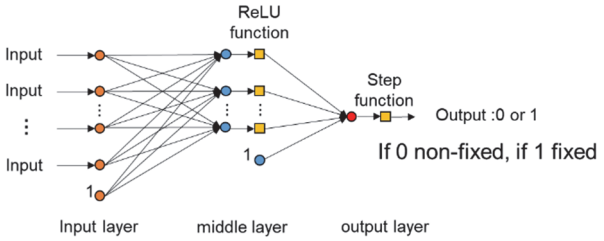

Figure 7. Schematic diagram of NN.

The formula for obtaining the output layer from the input layer through the middle layer is as follows:

$$\mathbf{m}_1 = \begin{bmatrix} \mathrm{ReLU}(\mathbf{W}_1\mathbf{x} + \mathbf{b}_1) \\ 1 \end{bmatrix}, \tag{7}$$

$$\mathbf{m}_j = \begin{bmatrix} \mathrm{ReLU}\left(\mathbf{W}_j\mathbf{m}_{j-1} + \mathbf{b}_j\right) \\ 1 \end{bmatrix} \ (j = 2, 3, \cdots, h) \tag{8}$$

$$\mathbf{y} = \mathbf{W}_{h+1}\mathbf{m}_h + \mathbf{b}_h \tag{9}$$

where $\mathbf{x}$ is an input vector, $\mathbf{W}_j$ is the jth weight matrix, $\mathbf{b}_j$ is the j-th bias, $\mathbf{m}_j$ is the j-th middle layer vector and $\mathbf{y}$ is an output vector. In this study, we compared the performance of two NNs. One is an "NN trained with error," and the other is "NN trained without error." Here, the number after "NN" in the name represents the number of nodes in the input, middle and output layers. In addition, "trained with error" and "trained without error" mean whether a displacement identification error is considered in the training of the NN or not, respectively; i.e., whether to use d_{Csim} or d_{sim} as the displacement of the instrument, both of which are presented in Section 5.2. The time interval at which the camera acquired one image was 0.033 s, hereafter referred as "1 step." NN36-12-4-1 input the posture information (displacement with or without identification error and the tipping angle of the instrument with casters) for up to 17 prior steps. In the output layer, output 1 or 0 indicates whether or not the caster is fixed, respectively.

6.2 Decision variables and evaluation functions of the switching control

The control was designed based on an optimization problem. We employed a decision vector $\mathbf{z}$ consisting of the elements of the weight matrix $\mathbf{W}$ of the NN and the objective function K, which is the maximum value of the instant evaluation value J in terms of time, t as follows:

$$\text{Minimize} \ \ K(\mathbf{z}) = \max_t J(\mathbf{z}, t) \tag{10}$$

$$\text{where} \ \ J(\mathbf{z}, t) = a_d \left(\frac{d(\mathbf{z},t)}{d_0}\right)^2 + a_\theta \left(\frac{\theta(\mathbf{z},t)}{\theta_0}\right)^2, \tag{11}$$

$d(\mathbf{z}, t)$ is the displacement at time t and $\theta(\mathbf{z}, t)$ is the tipping angle at time t. d_0 and θ_0 are dimensionless constants, and $a_d(=1)$ and $a_\theta(=1)$ the weighting coefficients for controlling the targets. Regarding the dimensionless constants, we adopt the largest value among $d_{\max}$ and $\theta_{\max}$ simulated in both cases where the instrument is constantly fixed and non-fixed under all the input waves in the training NN. In this study, the dimensionless constants used are d_0 (0.05477 m) and θ_0 (2.454°).

6.3 Reinforcement learning of the switching control

In this study, reinforcement learning of the switching control was performed, and an optimal weight matrix was calculated. Here, the decision variable was $\mathbf{z}$, and the objective function to be minimized is given by Eq. (10). To solve the optimization problem, we employed a genetic algorithm (GA) because local minima can appear in the optimization process. With respect to the parameters of GA, the number of individuals updated was set to 10, and the maximum number of generations was 400. The dynamic analysis for 20 s was performed 10 times in one generation, and this trial was repeated for 400 generations to obtain the optimal weight matrix. The number of design variables in NN36-12-4-1 was 501, which corresponds to the number of elements in the weight matrix.

In this study, the switching control learned by NN was considered the delay time of the proposed system, presented as t_d, t_i, t_c and t_s in Section 4.2. Considering the delay time of the camera and the calculation for identifying posture information, the posture information delayed by $t_i + t_c$ (0.308 s) from the behavior of the instrument with casters was input to the NN input layer. In addition, considering the delay time of the switching device, once switching was performed, there was a t_d (1.650 s) interval until the next switching.

A 5-story building model was created in accordance with the building model creation procedure described in Section 3.1, and the ground motion was input to obtain the acceleration response on the fifth floor. Figure 8 shows the time history wave for training the NN, which is the floor acceleration response to the earthquake motion prescribed by Notification No. 1461 of the Ministry of Construction, Japan, dated May 31, 2000. For the input wave for training NN, the time history of 0 to 20 s presented in Fig. 8 is used. In this study, we used the same 5-story building model for the input wave to validate the effectiveness of the proposed method.

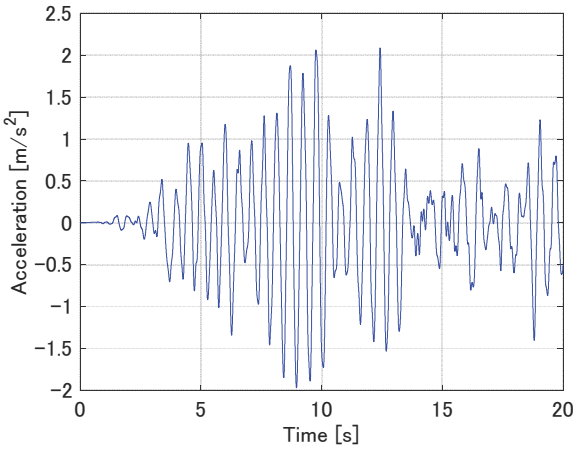

Figure 8. Time history of the floor acceleration response used in training NN.

Figure 9 shows the GA convergence of reinforcement learning performed using the floor response time history. The results show that it converged when number of generations was smaller than 400, which was the maximum number of generations used in this study. Therefore, a 400-generation NN is used in the following validity study.

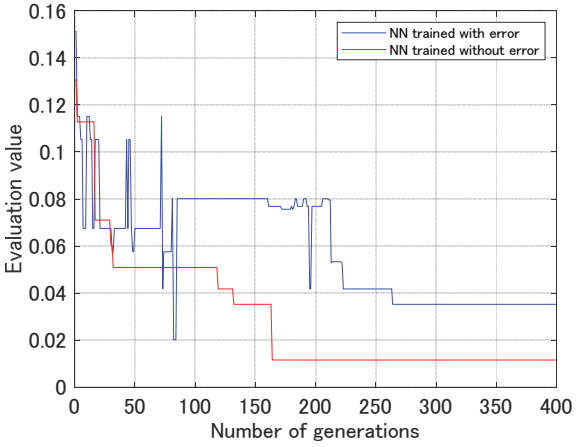

Figure 9. Convergence of reinforcement learning.

7. Validity study of the proposed control method

A dynamic analysis of the instrument with casters was performed to verify the effectiveness of the proposed control method "NN trained with error" We performed a dynamic analysis for four cases for a comparative study: two cases controlled using trained NNs and two cases constantly caster-fixed and non-fixed. The aforementioned design ground motion with a different Fourier phase spectrum from that used in the training NN shown in Fig. 8 was used for the validation study. Figure 10 shows the input wave used for validation, which is the floor acceleration response time history of the design ground motion. Figures 11–13 show the comparison of the evaluation value, displacement and tipping angle of the instrument with casters when the wave shown in Fig. 10 was input.

To confirm the effectiveness of the proposed method, we performed a dynamic analysis using 30 patterns of the aforementioned design ground motion with a Fourier phase spectrum different from that used in training NN, as shown in Fig. 8. Figure 14 shows a box plot of the maximum evaluation values for four cases in the 30 patterns of responses. Table 2 shows the comparison of the mean and standard deviation of the 30 evaluation values of the four cases. It shows that the mean and standard deviation of the proposed method (NN trained with error) are the smallest among the four cases.

In the experimental results, the switching control of "NN trained with error" reduced the response most, and the evaluation value was successfully reduced compared with the fixed and non-fixed conditions, confirming the effectiveness of the proposed method.

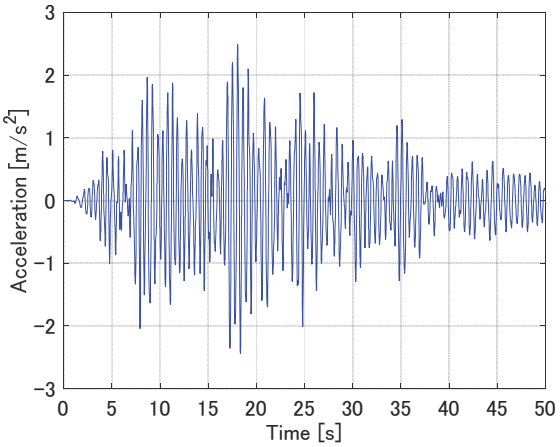

Figure 10. Floor acceleration response time history to design ground motion with a different Fourier phase spectrum from that used in training NN.

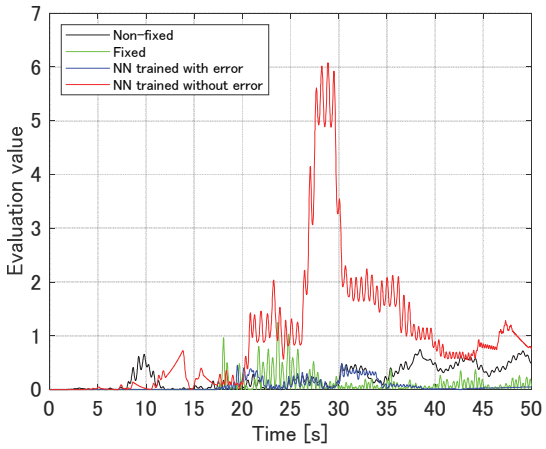

Figure 11. Comparison of time histories of the evaluation value.

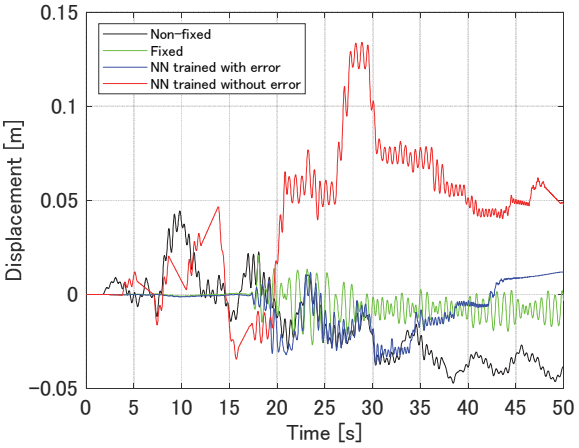

Figure 12. Comparison of the displacement time histories.

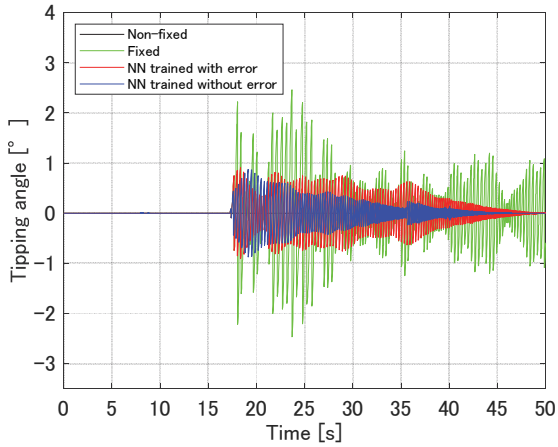

Figure 13. Comparison of the time histories of the tipping angle.

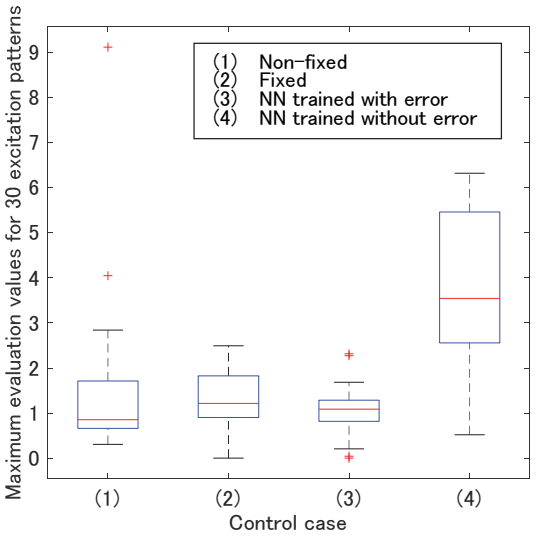

Figure 14. Distribution of the maximum evaluation values for 30 excitation patterns.

Table 2. Comparison of the means and standard deviations of the 30 evaluation values of four cases.

Control case	Mean	Standard deviation
Non-fixed	1.4424	1.6847
Fixed	1.3075	0.5813
NN trained with error	1.0599	0.5336
NN trained without error	3.6996	1.8210

8. Conclusions

We proposed to a seismic response control method for instruments with casters using computer vision and wireless communication and conducted experiments to verify the performance of the proposed method. We identified the stochastic models of the displacement measurement error of the instrument using computer vision. We considered the control delay of the proposed system and introduced stochastic models when constructing the control algorithm for switching the condition of casters. For switching control, NN reinforcement learning was employed, and control delay of the actual proposed system and stochastic models was introduced when performing dynamic analysis. Finally, to validate the proposed system, we performed a dynamic analysis of a controlled instrument subject to building floor motion. The "NN trained with error" with 36, 12, 4 and 1 layer nodes and posture information up to 1.06 times the fundamental natural period of the building input to the NN had the largest reduction effect. We confirmed that the instrument response was significantly suppressed by introducing the stochastic model of errors in the training of NN. This result suggests the usefulness of stochastic models to enhance the performance of reinforced learning based on dynamic simulations.

Acknowledgment

This work was supported by JSPS KAKENHI (Fundamental Research (B) Nos. 16H04455 and 20H02301).

References

Heslot, F., Baumberger, T., Perrin, B., Caroli, B. and Caroli, C. 1994. Creep, stick-slip, and dry-friction dynamics: Experiments and a heuristic model. *Physical Review E*, 49: 4973–4988.

Kawanishi, Y. and Kohiyama, M. 2018. Seismic response control for equipment with casters using switching wheel lock condition. In *Proceedings of the 13th World Congress on Computaional Mechanics and 2nd Pan American Congress on Computational Mechanics*,, July, 2018, *WCCM XIII and PANACM II,* New York, New York, July 22–27, 2018. IACM, pp. 132–143.

Saomoto, H. and Yoshimi, M. 2013. Seismic response simulation of furniture: Rational input including shape effect of building. *Journal of Japan Society of Civil Engineers, Ser. A1*, 69(4): I_642–I_649.

Wakabayashi, K., Kawanishi, Y., Kohiyama, M., Eguchi, R. and Takahashi, M. 2020. Seismic response control of an instrument with casters using computer vision based on reinforced learning of dynamic analysis results considering friction. *Journal of Structural Engineering*, 66B: 305–314.